BIOCHEMISTRY
including biophysical chemistry & molecular biology
Article

Biochemistry **2009,** *48,* 6299–6304 6299
DOI: 10.1021/bi900525v

Redox Properties of the Prosthetic Groups of Na^+-Translocating NADH:Quinone Oxidoreductase. 2. Study of the Enzyme by Optical Spectroscopy[†]

Alexander V. Bogachev,[‡] Dmitry A. Bloch,[§] Yulia V. Bertsova,[‡] and Michael I. Verkhovsky*[,§]

[‡]*Department of Molecular Energetics of Microorganisms, A. N. Belozersky Institute of Physico-Chemical Biology, Moscow State University, Moscow 119992, Russia, and* [§]*Institute of Biotechnology, P.O. Box 65 (Viikinkaari 1), University of Helsinki, Helsinki 00014, Finland*

Received March 27, 2009; Revised Manuscript Received May 27, 2009

ABSTRACT: Redox titration of the electronic spectra of the prosthetic groups of the Na^+-translocating NADH: quinone oxidoreductase (Na^+-NQR) from *Vibrio harveyi* at different pH values showed five redox transitions corresponding to the four flavin cofactors of the enzyme and one additional transition reflecting oxidoreduction of the [2Fe-2S] cluster. The pH dependence of the measured midpoint redox potentials showed that the two-electron reduction of the FAD located in the NqrF subunit was coupled with the uptake of only one H^+. The one-electron reduction of neutral semiquinone of riboflavin and the formation of anion flavosemiquinone from the oxidized FMN bound to the NqrB subunit were not coupled to any proton uptake. The two sequential one-electron reductions of the FMN residue bound to the NqrC subunit showed pH-independent formation of anion radical in the first step and the formation of fully reduced flavin coupled to the uptake of one H^+ in the second step. All four flavins stayed in the anionic form in the fully reduced enzyme. None of the six redox transitions in Na^+-NQR showed dependence of its midpoint redox potential on the concentration of sodium ions. A model of the sequence of electron transfer steps in the enzyme is suggested.

The Na^+-translocating NADH:quinone oxidoreductase (Na^+-NQR)[1] is a redox-driven sodium pump that generates transmembrane electrochemical Na^+ potential (*1*). This enzyme has been shown to operate in the respiratory chain of various bacteria, including several pathogenic microorganisms (*2*, *3*).

The enzyme consists of six subunits (NqrA−F) (*4*) encoded by the six genes of the *nqr* operon (*5*, *6*). Na^+-NQR is thought to contain the following set of prosthetic groups: one 2Fe-2S cluster (*7*, *8*), one noncovalently bound FAD (*7*), two covalently bound FMN residues (*9*), one noncovalently bound riboflavin (*10*, *11*), and one tightly bound ubiquinone-8 (*7*, *8*). Subunit NqrF possesses binding motifs for NADH, FAD, and [2Fe-2S] cluster (*5*, *12*, *13*), whereas covalently bound FMN residues are attached by phosphoester bonds to threonine residues in subunits NqrB and NqrC (*14*). However, there are no data on which subunit of Na^+-NQR riboflavin could bind to.

The kinetics of Na^+-NQR reduction by NADH displays several distinct phases corresponding to reduction of different flavin species, as shown by studies using stopped-flow optical spectroscopy (*8*, *15*). This reaction can be dissected into two parts with respect to the "coupling site" location. The first part (*before the coupling site*) is the sodium-independent fast hydride ion transfer from NADH to FAD and partial electron separation and the formation of equivalent fractions of reduced [2Fe-2S] cluster and neutral semiquinone of FAD (*16*). The second part (*after the coupling site*) consists of the phases that strongly depend on the sodium concentration. It was shown that the sodium-dependent phases reflect the reduction of (i) a neutral flavosemiquinone to the fully reduced flavin and (ii) an oxidized flavin to the anionic flavosemiquinone. Therefore, we have proposed that at least one of these one-electron transitions is coupled to the transmembrane sodium translocation by Na^+-NQR (*1*, *15*).

The mechanism of energy conversion between the redox transitions and the transmembrane translocation of a sodium ion is still unknown. It is only known that the reduction of Na^+-NQR is accompanied by ~1000-fold increase in its affinity to the coupling ion (the dissociation constant of Na^+ for the oxidized enzyme was found to be 24 mM and for the reduced enzyme about 30 μM) (*17*). Redox titration of all Na^+-NQR prosthetic groups at varied concentrations of Na^+ and at different pH values seems to be a necessary step in understanding the operating mechanism of the enzyme. This task has been done in the current work using spectropotentiometric redox titration.

[†]This work was supported by Biocentrum Helsinki (project number 7919028), the Sigrid Jusélius Foundation (project number 4700827), the Magnus Ehrnrooth Foundation, the Academy of Finland (project number 115108), and the Russian Foundation for Basic Research (project number 07-04-00619).

*To whom correspondence should be addressed. Phone: +358 9 191 58005. Fax: +358 9 191 58001. E-mail: michael.verkhovsky@helsinki.fi.

[1]Abbreviations: DDM, *n*-dodecyl-β-D-maltoside; E_m, midpoint redox potential; Fl, oxidized flavin; FlH_2, neutral form of reduced flavin; FlH^-, anionic form of reduced flavin; $FlH^\bullet$, neutral flavosemiquinone; $Fl^{\bullet-}$, anionic flavosemiquinone; Na^+-NQR, Na^+-translocating NADH: quinone oxidoreductase; Rf, riboflavin; SHE, standard hydrogen electrode; λ, wavelength.

Published on Web 06/04/2009

MATERIALS AND METHODS

Na^+-NQR from *Vibrio harveyi* was purified as described in ref (*18*).

Spectroelectrochemistry. Spectropotentiometric redox titration of Na^+-NQR was carried out using an optically transparent, thin-layer electrode cell as described in ref (*19*). Potentials within the range between −480 and +200 mV vs SHE were set with 20 mV steps during both oxidative and reductive titration using a PAR263A potentiostat (Princeton Applied Research). Optical absorption spectra were recorded in the spectral range of 350−770 nm at a succession of redox potentials. At each potential step, the onset of equilibrium on the working electrode was determined, as the changes in the cell current and optical density at 460 minus 560 nm became no longer significant (20−40 min per step). The titrations were performed at +21 °C.

To accelerate redox equilibrium between the working electrode surface and the solubilized enzyme molecules, 200 μM cobalt sepulchrate ($E_m = -350$ mV), 400 μM pentaamminechlororuthenium ($E_m = -130$ mV), and 200 μM hexaammineruthenium ($E_m = +50$ mV) were used as redox mediators. No optical contribution from the mediators was detected in the studied spectral range.

For the spectroelectrochemical experiments Na^+-NQR samples were washed with one of the following buffers, buffer A (100 mM KCl, 25 mM NaCl, 50 mM HEPES−Tris, pH 7.5, 0.1% DDM), buffer B (100 mM KCl, 50 mM HEPES−Tris, pH 7.5, 0.1% DDM), buffer C (100 mM KCl, 25 mM NaCl, 50 mM Bis-tris-propane−HEPES, pH 8.5, 0.1% DDM), or buffer D (100 mM KCl, 25 mM NaCl, 100 mM Bis-tris-propane−HEPES, pH 9.5, 0.1% DDM), and concentrated on centrifugal Amicon filters (100 kDa cutoff; Millipore) to ~50 μM enzyme. The sample (~40 μL) was supplemented with the mediators and used to fill the titration cell. All redox potentials quoted refer to SHE.

Protein content was determined by the bicinchoninic acid method using bovine serum albumin as a standard.

Sodium concentration was measured by flame photometry.

RESULTS

Redox Titration of Na^+-NQR Cofactors at Different pH Values. The absorption spectra of Na^+-NQR from *V. harveyi* were electrochemically titrated in the redox potential region from −480 to +200 mV (vs SHE) at different pH values. The pH range from 7.5 to 9.5 was limited by the stability of the protein during the relatively long titration procedure. The changes in the protein spectra upon reductive and oxidative titration were practically identical, and hysteresis at any step was less than 10 mV. For further analysis the spectra obtained under the same potentials in the oxidative and reductive directions were averaged.

Figure 1A represents the redox potential dependence of the optical density changes at each 20 mV oxidation step ($\Delta OD/\Delta E_h$) in the wavelength range from 350 to 770 nm at pH 8.5. As it is clearly seen from the figure, this dependence has a rather large number of the peaks and troughs reflecting midpoint redox potentials of Na^+-NQR redox cofactors. One peak at −231 mV is narrow with half-width of ~44 mV, which is characteristic for a two-electron redox transition. All the other peaks have half-width of ~88 mV, typical for one-electron transitions. Figure 1B shows decomposition of the experimental points at 490 nm, where all redox cofactors have absorbance, into individual redox transitions (dashed lines). The solid line represents the sum of all individual transitions and fits the data well.

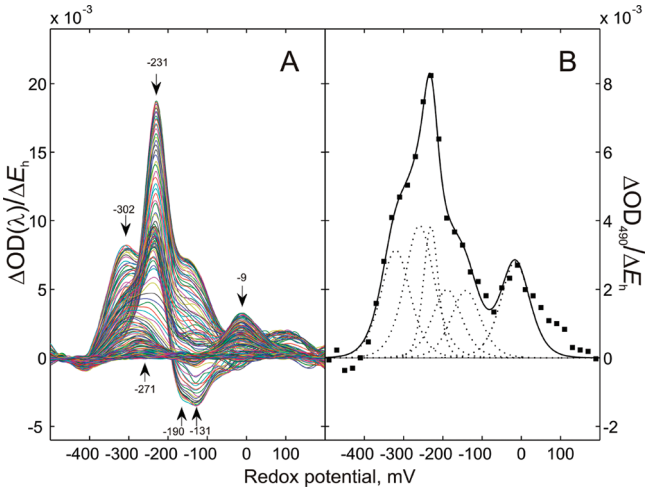

FIGURE 1: Redox potential dependence of optical density changes ($\Delta OD/\Delta E_h$) in Na^+-NQR upon 20 mV step oxidation. (A) The OD taken every 2 nm in the wavelength range from 350 to 770 nm. (B) The OD taken at 490 nm. Arrows with numbers represent the positions of the maxima and minima corresponding to the values of the midpoint redox potential of different cofactors. Shown in (B) is the fit (solid line) through the experimental points at 490 nm where all known cofactors have absorbance. The dotted lines show content of each transition from six found in the fit. The pH of the titration medium was 8.5. For other conditions, see Materials and Methods.

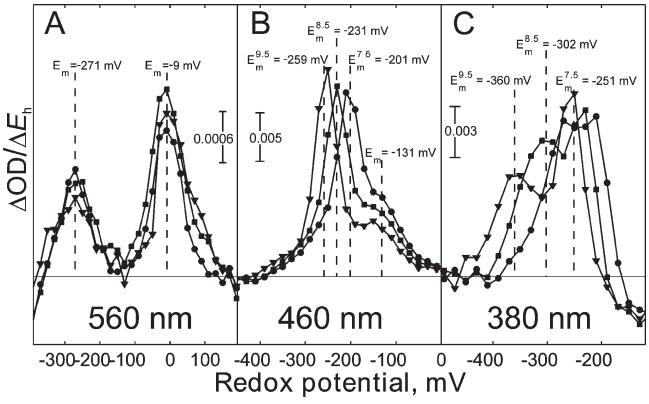

FIGURE 2: Redox potential dependence of $\Delta OD/\Delta E_h$ taken at different wavelengths: (A) 560 nm; (B) 460 nm; (C) 380 nm. The pH values are (●) 7.5, (■) 8.5, and (▼) 9.5. Other conditions as for Figure 1.

To show clearly the pH dependence of the midpoint potentials (maxima in our plots) of the different enzyme cofactors, the $\Delta OD/\Delta E_h$ titration profiles are presented at different pHs (Figure 2). Figure 2A represents data obtained in the long-wavelength region (λ = 560 nm) where only the [2Fe-2S] cluster and neutral flavosemiquinone ($FlH^\bullet$) have absorbance (*19*). In this figure the two well-separated peaks reflecting the [2Fe-2S] cluster oxidation ($E_m = -271$ mV) (*8*) and the formation of $FlH^\bullet$ from fully reduced flavin ($E_m = -9$ mV) (*18*) are clearly seen. As expected, the redox transition of the [2Fe-2S] cluster does not show any dependence on pH, and all "−271 mV" peaks at pH 7.5, 8.5, and 9.5 coincide. More surprisingly, the formation of the neutral flavosemiquinone from the reduced flavin (the "−9 mV" peak) shows no pH dependence either. This is possible if the fully reduced flavin exists in the anionic form; thus this transition can be described as $FlH^- \leftrightarrow FlH^\bullet$ ($1e^-$). It is noteworthy that an alternative explanation of the absence of pH dependence is also possible, if the flavin anion is neutralized by the proton from an

amino acid residue that is not in contact with the bulk phase. In any case the absence of pH dependence implies that $FlH^{\bullet}$ reduction leads to appearance of 1-equivalent of uncompensated negative charge in Na^+-NQR.

Figure 2B shows the $\Delta OD/\Delta E_h$ dependence at 460 nm where the oxidized form of flavins has an absorption maximum (*19*). At pH 7.5 a sharp peak (E_m=−201 mV, n=2) reflecting two-electron flavin transition is well seen (*19*). Alkalinization leads to the shift in its position to the negative potentials with dependence close to −30 mV/pH unit. Thus, full two-electron reduction of this flavin results in uptake of only one proton, and the reaction can be described as $FlH^- \leftrightarrow Fl$ ($2e^-$, $1H^+$). The graphs in Figure 2B also have other wider peaks corresponding to single-electron flavin reduction (for example, with $E_m = -131$ mV) that do not depend on pH.

Figure 2C shows the data at λ = 380 nm, where a significant contribution from the anionic forms of flavosemiquinone (*19*) in the spectra can be seen. These curves contain several components, but only one of them is pH-dependent and its E_m is shifted by −60 mV per pH unit. At pH 9.5 this transition has $E_m = -360$ mV, which is more negative than any other redox transitions in the enzyme. This property gives us a possibility to obtain the pure optical spectrum of the transition, which is shown in Figure 3 as "FlH^- *minus* $Fl^{\bullet -}$". The presented spectrum is characteristic for the formation of the anionic flavosemiquinone form from the fully reduced flavin (*15*, *19*), and since the reduction of the anionic flavosemiquinone results in the uptake of a single proton the reaction can be described as $FlH^- \leftrightarrow Fl^{\bullet -}$ ($1e^-$, $1H^+$).

In the previous study of the redox properties of Na^+-NQR (*19*) the thermodynamic properties of only three flavin cofactors of the protein were defined. One of them was found to operate as a two-electron carrier with $E_m^{7.5}$ of −200 mV. Each of two others was capable solely of one-electron reduction: one from neutral flavosemiquinone to fully reduced flavin (E_m = +20 mV) and the other from oxidized flavin to flavosemiquinone anion (E_m = −150 mV) (*19*). However, as shown in the accompanying paper (*18*), the titration of Na^+-NQR at pH 7.5 using EPR spectroscopy elicited two more transitions, as with E_m = −190 mV and E_m = −275 mV. These transitions reflect the formation and disappearance of a radical signal, respectively. From the optical titration presented here, it follows that the transition with $E_m^{7.5} \approx -275$ mV describes the formation of the *anion* flavosemiquinone from the fully reduced flavin, thus the second transition with $E_m^{7.5} \approx -190$ mV should correspond to the oxidation of this anion flavosemiquinone to the fully oxidized form of the flavin ($Fl^{\bullet -} \leftrightarrow Fl$ ($1e^-$)).

As a result, the redox titration of Na^+-NQR brought out five redox transitions of four different flavin cofactors (see Table 1): $Fl_1H^- \leftrightarrow Fl_1$ ($2e^-$, $1H^+$), $Fl_2H^- \leftrightarrow Fl_2^{\bullet -}$ ($1e^-$, $1H^+$), $Fl_2^{\bullet -} \leftrightarrow Fl_2$ ($1e^-$), $Fl_3^{\bullet -} \leftrightarrow Fl_3$ ($1e^-$), and $Fl_4H^- \leftrightarrow Fl_4H^{\bullet}$ ($1e^-$), as well as a transition of the [2Fe-2S] cluster. The enzyme preparation also contains a tightly bound ubiquinone-8, which undergoes two-electron transition with expected potential of about +100 mV, but the absence of absorbance in the visible region did not allow us to define its exact midpoint potential. The semiquinone form of this quinone was not observed either by EPR (*18*) or by the optical titration.

We have obtained a set of "model" electronic spectra for all of the redox transitions mentioned above (Figure 3). The spectrum of the $Fl_1H^- \leftrightarrow Fl_1$ ($2e^-$, $1H^+$) transition was modeled by anaerobic reduction of glucose oxidase in the presence of glucose (*15*). The spectrum of the $Fl_2H^- \leftrightarrow Fl_2^{\bullet -}$ ($1e^-$, $1H^+$)

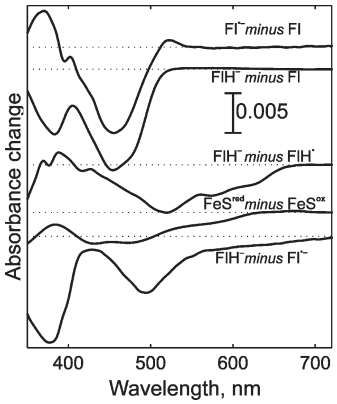

FIGURE 3: A set of reduced minus oxidized spectra for all redox transitions in the enzyme. The ΔA = 0 level is shown by dotted lines for each spectrum. The region around about 700 nm was selected as a reference where none of the transition has an absolute absorbance. All spectra correspond to 1 μM concentration of the enzyme.

Table 1

cofactor	redox transition	$E_m^{7.5}$, mV	no. of electrons	pH dependence	$[Na^+]$ dependence
FAD_{NqrF}	$Fl_1H^- \leftrightarrow Fl_1$	−200	2	−30 mV/pH	no
FMN_{NqrC}	$Fl_2H^- \leftrightarrow Fl_2^{\bullet -}$	−250	1	−60 mV/pH	no
FMN_{NqrC}	$Fl_2^{\bullet -} \leftrightarrow Fl_2$	−200	1	no	no
FMN_{NqrB}	$Fl_3^{\bullet -} \leftrightarrow Fl_3$	−130	1	no	no
$Rf_{Nqr?}$	$Fl_4H^- \leftrightarrow Fl_4H^{\bullet}$	−10	1	no	no
$[2Fe\text{-}2S]_{NqrF}$	$[2Fe\text{-}2S]^+ \leftrightarrow [2Fe\text{-}2S]^{2+}$	−270	1	no	no

transition was obtained from the analysis of the optical changes at the pH = 9.5 titration in the low potential region (see above). The same analysis in the redox potential range from −120 to −80 mV gave the pure spectrum of $Fl_3^{\bullet -} \leftrightarrow Fl_3$ ($1e^-$) (see also ref (*19*)). It is important to mention that the sum of the observed spectra for the two transitions $Fl_2H^- \leftrightarrow Fl_2^{\bullet -}$ ($1e^-$, $1H^+$) and $Fl_3^{\bullet -} \leftrightarrow Fl_3$ ($1e^-$) does not represent a typical spectrum of two-electron flavin reduction. From this observation we concluded that these two transitions come from different flavin cofactors. The found earlier (*19*) $Fl^{\bullet -} \leftrightarrow Fl$ ($1e^-$) transition with the $E_m^{7.5}$ = −131 mV describes the redox event of Fl_3, and the same transition with the E_m = −190 mV (*18*) belongs to Fl_2. Owing to the strong overlap of the electronic (optical) spectra in the region of the redox potentials around −200 mV, we could not extract a pure spectrum for $Fl_2^{\bullet -} \leftrightarrow Fl_2$ ($1e^-$). However, this transition has the same chemical nature as the $Fl_3^{\bullet -} \leftrightarrow Fl_3$ ($1e^-$) reaction, and we can assume that they have similar spectra. Thus, as a model of these two transitions we used the same spectrum presented in Figure 3. The spectrum of the redox transition for the last, fourth flavin $Fl_4H^- \leftrightarrow Fl_4H^{\bullet}$ ($1e^-$) can be easily found because it represents the only transition in the potential region from −30 to +10 mV (see also ref (*19*)). As a model of the transition spectrum for $[2Fe\text{-}2S]^+ \leftrightarrow [2Fe\text{-}2S]^{2+}$ we used the spectrum obtained from the isolated fragment of Na^+-NQR containing [2Fe-2S] cluster described in ref (*12*). In Figure 3 all spectra are normalized for 1 μM enzyme. The thermodynamic characteristics found in this and the accompanying paper (*18*) and presented in Table 1 together with the spectra from Figure 3 allowed us to obtain the model titration surface. This surface at pH 7.5 is shown together with the experimental data in Figure 4. As can be seen, the model surface is very similar to the experimental one. It is very important to mention that our approach very well

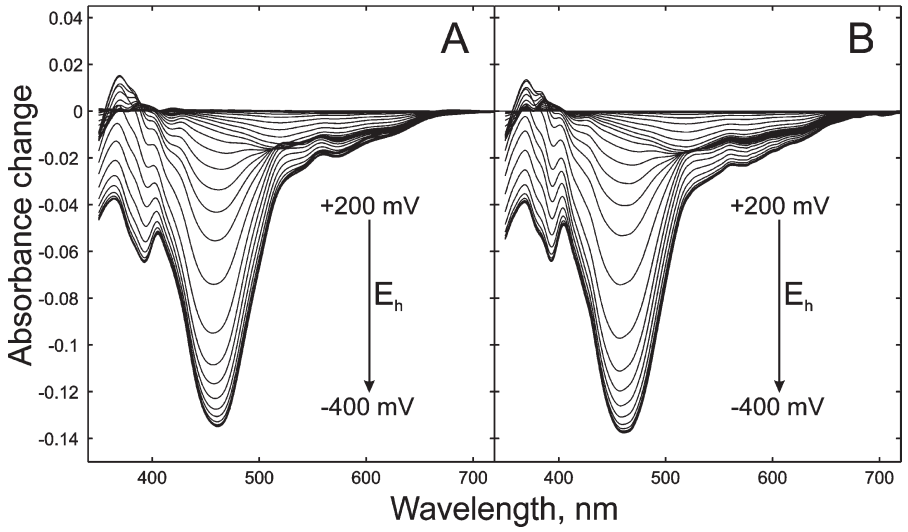

FIGURE 4: (A) Difference spectral surface (different level of reduction minus oxidized) of Na^+-NQR obtained during the spectroelectrochemical redox titration at redox potentials from +200 to −400 mV with the step of 20 mV and (B) the theoretical surface obtained from the set of spectra presented in Figure 3 and the redox behavior of the enzyme transitions with midpoint potentials presented in Table 1. In (A) the spectrum at +200 mV was used as the reference. The optical path length was 0.6 mm. The data are for pH 7.5. For other conditions, see Materials and Methods.

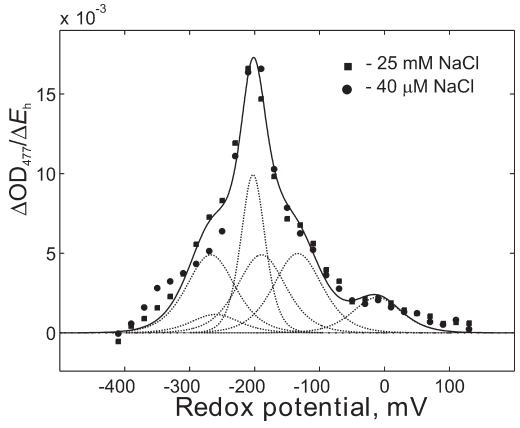

FIGURE 5: $\Delta OD/\Delta E_h$ taken at 477 nm at different Na^+ concentrations: (●) 40 μM; (■) 25 mM. The solid line through the experimental points at 477 nm shows the fit. The dotted lines show the content of each transition from the six found in the fit of the data at pH = 7.5.

modeled the experimental data at all pH values used (data not shown).

The quality of the fit at pH 8.5 also can be seen from Figure 1B: the theoretical solid curve passes through the experimental points at λ = 490 nm, where all six cofactors have their absorbance. The small deviation of the theoretical curve from the data in the high-potential region is connected with the presence of a small cytochrome *c* contamination.

Effect of Sodium Ion Concentration on Midpoint Redox Potentials of Na^+-NQR Cofactors. In the previous work (*19*) we found that the thermodynamic parameters of three flavin cofactors and also one [2Fe-2S] cluster of Na^+-NQR do not depend on Na^+ concentration. In this investigation by optical (the present paper) and EPR (accompanying paper) spectroscopy we discovered two additional redox transitions for the fourth flavin cofactor of the enzyme. To reveal the mechanism of the coupling between ion transport and electron transfer, it is very important to find out whether the values of midpoint potentials for these new transitions depend on sodium concentration.

Figure 5 demonstrates that the positions of all six found redox transitions show no shift upon ~1000-fold increase in sodium concentration. Only the $[2Fe\text{-}2S]^+ \leftrightarrow [2Fe\text{-}2S]^{2+}$ transition exhibits a small change of its E_m upon rise of $[Na^+]$. However, this effect is so small in comparison to the expected dependence of −60 mV per 10-fold decrease of sodium concentration that we can conclude that the midpoint redox potentials of all redox transitions tested are practically sodium-independent.

Extinction Coefficients of Na^+-NQR. The obtained model of all redox transitions of Na^+-NQR allowed us to calculate the molar extinction coefficients for the different enzyme states. For oxidized Na^+-NQR, $\varepsilon_{465-520} = 43.4\ mM^{-1}\ cm^{-1}$; for the reduced minus oxidized Na^+-NQR spectrum, $\varepsilon_{465-770} = 44.3\ mM^{-1}\ cm^{-1}$ and $\varepsilon_{465-520} = 31.8\ mM^{-1}\ cm^{-1}$.

DISCUSSION

In the present and accompanying (*18*) works we have performed redox titration of all the redox cofactors of Na^+-NQR that have absorbance in the visible spectral region and/or can be detected by EPR spectroscopy: four flavins and one 2Fe-2S cluster. For the four flavins we defined all transitions possible at equilibrium conditions and found that there are five of them. As we have mentioned in the Introduction, Na^+-NQR contains one FAD, two covalently bound FMN, and one noncovalently attached riboflavin. Which of these flavins has particular thermodynamic properties found in our investigation?

The first one (Fl_1) was found to operate as a two-electron carrier with $E_m^{7.5}$ of −200 mV. Our previous data (*15*, *19*) let us assign this two-electron $Fl_1H^- \leftrightarrow Fl_1$ ($2e^-$) transition to the reduction of noncovalently bound FAD in the NADH dehydrogenase domain of Na^+-NQR located in the NqrF subunit (see Table 1). It is noteworthy that full reduction of FAD at neutral pH is coupled with the uptake of only one proton, and the reduced cofactor under these conditions stays in the anionic form.

It is relatively easy to assign Fl_4 because it is capable solely of the one-electron transition from neutral flavosemiquinone to fully reduced flavin with $E_m = -10$ mV. Therefore, this is the flavin which is responsible for the presence of the *neutral* flavin radical in the fully *oxidized* enzyme (*15*, *20*). Recently, it has been shown that this unique property of Na^+-NQR is defined by the

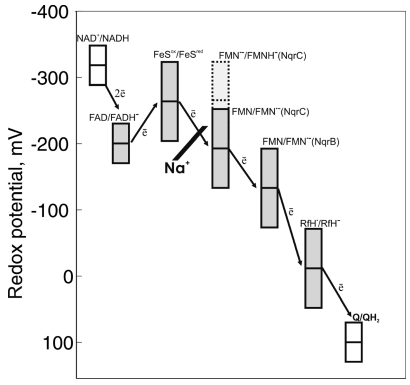

FIGURE 6: Scheme of the redox transitions of Na^+-NQR cofactors and possible sequence of electron transfer from NADH to ubiquinone. The energy levels of the enzyme cofactors are presented by the boxes. The middle of each box represents the midpoint potential at pH = 7.5, and the height of it points out the reduction level from 10% to 90%.

presence of riboflavin (*11*). Thus, the redox transition for Fl_4 with $E_m = -10$ mV belongs to a riboflavin species ($RfH^- \leftrightarrow RfH^\bullet$ ($1e^-$)). Again, we should point out that the fully reduced riboflavin at neutral pH stays in the anionic form.

Flavin 3 is also capable of only one-electron transition, but in this case the transition is from the oxidized flavin to the flavosemiquinone anion ($E_m = -130$ mV). This is the flavin responsible for the presence of the *anionic* flavosemiquinone radical signal in the fully *reduced* enzyme (*15*, *20*). It was established (*21*) that this unusual property of Na^+-NQR is connected to the FMN residue covalently bound to threonine [T235] of the NqrB subunit. Therefore, the transition with the $E_m = -130$ mV of Fl_3 can be written as $FMN_{NqrB}^{\bullet -} \leftrightarrow FMN_{NqrB}$ ($1e^-$).

The last flavin (Fl_2) capable of two sequential one-electron reduction steps $Fl_2^{\bullet -} \leftrightarrow Fl_2$ ($1e^-$) and $Fl_2H^- \leftrightarrow Fl_2^{\bullet -}$ ($1e^-$) with $E_{m1}^{7.5} = -200$ mV and $E_{m2}^{7.5} = -250$ mV can be identified as the FMN residue covalently bound to threonine [T229] of the NqrC subunit (also see ref (*21*)) by exclusion. This flavin as well as all others stays in the enzyme in anionic form upon complete reduction.

All properties of assigned redox transitions for the known enzyme prosthetic groups are summarized in Table 1.

Summarizing the sequence analysis of the Na^+-NQR subunits (*5*, *12*), the kinetics of the enzyme reduction by NADH (*15*, *16*), the thermodynamic properties of its cofactors (present work), measured distance between the Na^+-NQR prosthetic groups (*18*), and mutagenesis studies (*22*), a plausible scheme of electron transport within Na^+-NQR during its turnover can be suggested (Figure 6). It implies that initially hydride ion from NADH is transferred to the noncovalently bound FAD. Then the electrons are separated, resulting in a FAD semiquinone and reduced [2Fe-2S] cluster (*16*). An electron from the FeS cluster should be further transferred to covalently bound FMN residues. Since the measured distance between [2Fe-2S] cluster and FMN_{NqrB} is too large for a direct electron transfer (*18*), we can assume that the electron from the FeS cluster is transferred first to the FMN_{NqrC} and only then to FMN_{NqrB} (see Figure 6). As riboflavin is the center with the highest potential in Na^+-NQR, we propose that this is the center that is located at the end of the electron transfer chain of the enzyme and passes the electrons to ubiquinone. This location of the riboflavin has also been corroborated by the recent mutagenesis work (*22*). Surprisingly, the drop of the midpoint redox potentials in the chain of the cofactors is rather smooth. There is no clear spot in the chain where the major portion of energy for coupling to the ion translocation could be released, as in the case of, e.g., Complex I, where the major energy drop of about 350 mV occurs between N2 cluster and ubiquinone, the point of the proposed coupling site (*23*).

It is noteworthy that all flavin cofactors in the reduced form of the Na^+-NQR were found to be negatively charged, and this means that there is rather large electrostatic repulsion, which should influence their redox potentials. It is plausible that in the kinetic mode of the enzyme action and electron transfer the neighbor cofactor(s) would be oxidized and the *functional* redox potentials can be quite different from the *equilibrium* potentials found in this work. We already have obtained clear indication of this phenomenon: during fast kinetic measurements Na^+-NQR reaches states that are not accessible under equilibrium conditions (*16*). At the same time, the knowledge of the thermodynamic properties of all cofactor creates the framework for the model of the possible redox transitions during the turnover of the enzyme.

REFERENCES

1. Bogachev, A. V., and Verkhovsky, M. I. (2005) Na^+-translocating NADH:quinone oxidoreductase: progress achieved and prospects of investigations. *Biochemistry (Moscow) 70*, 143–149.
2. Zhou, W., Bertsova, Y. V., Feng, B., Tsatsos, P., Verkhovskaya M. L., Gennis, R. B., Bogachev, A. V., and Barquera, B. (1999) Sequencing and preliminary characterization of the Na^+-translocating NADH:ubiquinone oxidoreductase from *Vibrio harveyi*. *Biochemistry 38*, 16246–16252.
3. Hase, C. C., Fedorova, N. D., Galperin, M. Y., and Dibrov, P. A. (2001) Sodium ion cycle in bacterial pathogens: evidence from cross-genome comparisons. *Microbiol. Mol. Biol. Rev. 65*, 353–370.
4. Nakayama, Y., Hayashi, M., and Unemoto, T. (1998) Identification of six subunits constituting Na^+-translocating NADH-quinone reductase from the marine *Vibrio alginolyticus*. *FEBS Lett. 422*, 240–242.
5. Rich, P. R., Meunier, B., and Ward, F. B. (1995) Predicted structure and possible ionmotive mechanism of the sodium-linked NADH-ubiquinone oxidoreductase of *Vibrio alginolyticus*. *FEBS Lett. 375*, 5–10.
6. Hayashi, M., Hirai, K., and Unemoto, T. (1995) Sequencing and the alignment of structural genes in the nqr operon encoding the Na^+-translocating NADH-quinone reductase from *Vibrio alginolyticus*. *FEBS Lett. 363*, 75–77.
7. Pfenninger-Li, X. D., Albracht, S. P., van Belzen, R., and Dimroth, P. (1996) NADH:ubiquinone oxidoreductase of *Vibrio alginolyticus*: purification, properties, and reconstitution of the Na^+ pump. *Biochemistry 35*, 6233–6242.
8. Bogachev, A. V., Bertsova, Y. V., Barquera, B., and Verkhovsky, M. I. (2001) Sodium-dependent steps in the redox reactions of the Na^+-motive NADH:quinone oxidoreductase from *Vibrio harveyi*. *Biochemistry 40*, 7318–7323.
9. Nakayama, Y., Yasui, M., Sugahara, K., Hayashi, M., and Unemoto, T. (2000) Covalently bound flavin in the NqrB and NqrC subunits of Na^+-translocating NADH-quinone reductase from *Vibrio alginolyticus*. *FEBS Lett. 474*, 165–168.
10. Barquera, B., Zhou, W., Morgan, J. E., and Gennis, R. B. (2002) Riboflavin is a component of the Na^+-pumping NADH-quinone oxidoreductase from *Vibrio cholerae*. *Proc. Natl. Acad. Sci. U.S.A. 99*, 10322–10324.
11. Juárez, O., Nilges, M. J., Gillespie, P., Cotton, J., and Barquera, B. (2008) Riboflavin is an active redox cofactor in the Na^+-pumping NADH:quinone oxidoreductase (Na^+-NQR) from *Vibrio cholerae*. *J. Biol. Chem. 283*, 33162–33167.
12. Turk, K., Puhar, A., Neese, F., Bill, E., Fritz, G., and Steuber, J. (2004) NADH oxidation by the Na^+-translocating NADH:quinone oxidoreductase from *Vibrio cholerae*: functional role of the NqrF subunit. *J. Biol. Chem. 279*, 21349–21355.
13. Barquera, B., Nilges, M. J., Morgan, J. E., Ramirez-Silva, L., Zhou, W., and Gennis, R. B. (2004) Mutagenesis study of the 2Fe-

2S center and the FAD binding site of the Na^+-translocating NADH: ubiquinone oxidoreductase from *Vibrio cholerae*. *Biochemistry 43*, 12322–12330.
14. Hayashi, M., Nakayama, Y., Yasui, M., Maeda, M., Furuishi, K., and Unemoto, T. (2001) FMN is covalently attached to a threonine residue in the NqrB and NqrC subunits of Na^+-translocating NADH-quinone reductase from *Vibrio alginolyticus*. *FEBS Lett. 488*, 5–8.
15. Bogachev, A. V., Bertsova, Y. V., Ruuge, E. K., Wikström, M., and Verkhovsky, M. I. (2002) Kinetics of the spectral changes during reduction of the Na^+-motive NADH:quinone oxidoreductase from *Vibrio harveyi*. *Biochim. Biophys. Acta 1556*, 113–120.
16. Bogachev, A. V., Belevich, N. P., Bertsova, Y. V., and Verkhovsky, M. I. (2009) Primary steps of Na^+-translocating NADH:ubiquinone oxidoreductase catalytic cycle resolved by the ultra-fast freeze-quench approach. *J. Biol. Chem. 284*, 5533–5538.
17. Bogachev, A. V., Bertsova, Y. V., Aitio, O., Permi, P., and Verkhovsky, M. I. (2007) Redox-dependent sodium binding by the Na^+-translocating NADH:quinone oxidoreductase from *Vibrio harveyi*. *Biochemistry 46*, 10186–10191.
18. Bogachev, A. V., Kulik, L. V., Bloch, D. A., Bertsova, Y. V., Fadeeva, M. S., and Verkhovsky, M. I. (2009) Redox properties of the prosthetic groups of Na^+-translocating NADH:quinone oxidoreductase. 1. Electron paramagnetic resonance study of the enzyme, *Biochemistry* (DOI 10.1021/bi900524m).
19. Bogachev, A. V., Bertsova, Y. V., Bloch, D. A., and Verkhovsky, M. I. (2006) Thermodynamic properties of the redox centers of Na^+-translocating NADH:quinone oxidoreductase. *Biochemistry 45*, 3421–3428.
20. Barquera, B., Morgan, J. E., Lukoyanov, D., Scholes, C. P., Gennis, R. B., and Nilges, M. J. (2003) X- and W-band EPR and Q-band ENDOR studies of the flavin radical in the Na^+ -translocating NADH:quinone oxidoreductase from *Vibrio cholerae*. *J. Am. Chem. Soc. 125*, 265–275.
21. Barquera, B., Ramirez-Silva, L., Morgan, J. E., and Nilges, M. J. (2006) A new flavin radical signal in the Na^+-pumping NADH: quinone oxidoreductase from *Vibrio cholerae*. An EPR/electron nuclear double resonance investigation of the role of the covalently bound flavins in subunits B and C. *J. Biol. Chem. 281*, 36482–36491.
22. Juárez, O., Morgan, J. E., and Barquera, B. (2009) The electron transfer pathway of the Na^+-pumping NADH:quinone oxidoreductase from *Vibrio cholerae*. *J. Biol. Chem. 284*, 8963–8972.
23. Euro, L., Bloch, D. A., Wikström, M., Verkhovsky, M. I., and Verkhovskaya, M. (2008) Electrostatic interactions between FeS clusters in NADH:ubiquinone oxidoreductase (Complex I) from *Escherichia coli*. *Biochemistry 47*, 3185–3193.